Australian Meteorological and Oceanographic Journal 59 (2010) 77-86

Including a new data stream in the BLUElink Ocean Data Assimilation System

Isabel Andreu-Burillo[1,2], Gary Brassington[1,2], Peter Oke[1,3] and Helen Beggs[1,2]

[1]Centre for Australian Weather and Climate Research - a partnership between CSIRO and the Bureau of Meteorology, Australia
[2]Bureau of Meteorology, Melbourne, Australia
[3]CSIRO Marine and Atmospheric Research and Wealth from Oceans Flagship Program, Hobart, Australia

A satellite-derived sea-surface temperature (SST) data stream has been recently added to the BLUElink Ocean Data Assimilation System (BODAS) with the purpose of increasing its robustness.

This paper presents the new data-set as well as the pre-existing data stream. We also assess the impact of their assimilation through two sets of analyses that make use of each data-set separately, and a third that assimilates a combination of both. The new data stream brings in higher accuracy and resolution which can constrain closer to the coast. Results show an improvement of the analysis over the background states in all cases. Combining the two data streams brings analyses closer to buoy observations than assimilation of the data streams separately.

Introduction

BLUElink (Brassington et al. 2007) is a Bureau of Meteorology, CSIRO and Royal Australian Navy project intended to deliver ocean forecasts for the Australian region. The project has been implemented through its Ocean Model Analysis and Prediction System (OceanMAPS), with the Ocean Forecasting Australia Model (OFAM) as the modelling component and the BLUElink Ocean Data Assimilation System (BODAS) as the (re-)analysis component.

BODAS (Oke et al. 2008) is an Ensemble Optimal Interpolation (EnOI) scheme capable of producing multivariate analyses using single or multiple observation sources such as satellite sea-surface temperature (SST), altimetry data and *in situ* temperature and salinity profiles.

Recently, a new SST data stream has been included in BODAS. One of the main motivations for this was to increase the robustness of the analysis system by having two SST observation streams, with the possibility of reassessing the quality of the pre-existing SST data stream as an outcome. The new SST data stream comes from the US Naval Oceanographic Office's Global Area Coverage Advanced Very High Resolution Radiometer level 2 product (NAVOCEANO's GAC AVHRR L2P SST), which does not provide observations through clouds but contains useful observations closer to the coast, and with higher resolution, than the already used AMSR-E (Advanced Microwave Scanning Radiometer – Earth Observing System) data-set. The latter is obtained from a microwave sensor and can see through clouds, but not in rain. AMSR-E is also affected by ocean-surface roughness. Combination of the two data-sets should result in a better assessment of their information content and improved global coverage.

This paper presents the processing of NAVOCEANO's GAC AVHRR L2P SST for use in BODAS, the characteristics of this data-set and of the already used AMSR-E data-set, together with some results of their assimilation using BODAS, for February 2008.

We briefly introduce the thermal structure of the upper ocean, the physics underlying satellite SST measurements and what our prediction systems are able to represent. Next, NAVOCEANO's GAC AVHRR L2P SST product is presented, and compared to buoy observations, as are the AMSR-E descending data. We then present some results of the assimilation experiments conducted using the new data stream and its combination with the previously available data stream. Discussion and conclusions follow.

Corresponding author address: Isabel Andreu-Burillo, Bureau of Meteorology, GPO Box 1289, Melbourne, Vic. 3001, Australia.
Email: I.Andreu-Burillo@bom.gov.au

Thermal structure in the upper ocean

We will refer to the upper ocean or near-surface layer of the ocean as the transition zone between the atmospheric boundary layer and the deep ocean. The dominant dynamical processes in this zone result from the combination of local fluxes of heat, moisture, momentum and gas from the atmosphere, giving rise to various sublayers with different governing mechanisms and regimes. The strong dependence of the mixing regime below the air-sea interface upon meteorological, radiation and surface wave conditions makes it impossible to give a universal definition of this layer in metres (Soloviev and Lukas 2006), with some processes being confined to the first few millimetres, others with scales of tens of metres.

Figure 1 is a qualitative representation of the temperature structure in the upper ocean under light winds (up to 6 m/s) and strong solar radiation. During daytime, solar radiation causes warming throughout a depth of ~10 m. Here, the temperature profile shows a diurnal cycle with progressive warming, starting at the surface, from sunrise, a peak of highest temperatures in the afternoon and minimum temperatures just before dawn, when the temperature is quasi-homogeneous within this part of the water column. This uniform temperature, which varies at time-scales longer than a day, is referred to as the foundation temperature and notated T_{fnd}.

The top millimetres of the ocean surface are subject to strong thermal variations, involving a range of processes with short space and time-scales. This layer is often referred to as the sea-surface micro-layer. It presents features that are not resolved by ocean forecast systems, but need to be taken into account in the retrieval of observations for forecast purposes, as it is within this layer that remote sensing measures ocean temperatures.

Radiometers measure the temperature, SST_{skin}, in the skin layer, situated within a few micrometres from the ocean surface. Microwave devices detect temperatures close to the subskin temperature ($SST_{subskin}$), within a few millimetres from the air-sea interface.

The Group for High-Resolution Sea Surface Temperature (GHRSST) portal (http://www.ghrsst-pp.org/SST-Definitions.html) provides some information on the vertical structure of surface temperature. A thorough presentation on the near-surface ocean and processes involved is given by Soloviev and Lukas (2006).

As mentioned above, this description corresponds to a situation of light winds. For sustained wind conditions (above 6 m/s and below 22 m/s), the mixing produced by the stirring would homogenise temperatures in the top of the water column, resulting in a temperature that could be identified as foundation even during daytime.

OceanMAPS represents the ocean fields with a resolution of 10 m in the surface layers. Sea-surface temperature observations intended for assimilation within this system will therefore need to represent a temperature corresponding to the upper 10 m of the water column.

The next section will present the pre-processing of NAVOCEANO's GAC AVHRR L2P SST product in order to produce a new data stream to be assimilated through the analysis component of OceanMAPS: the BLUElink Ocean Data Assimilation System (BODAS).

NAVOCEANO's GAC AVHRR L2P SST

Our choice for the data stream to be incorporated into BODAS has been that of a GHRSST level 2 product (L2P). Level 2 files produced according to GHRSST specifications include SST data as delivered by the data provider in their native format, together with a number of ancillary fields. In the case

Fig. 1 Schematic of the SST definitions adopted by the Group for High Resolution SST (GHRSST) to help distinguish diurnal effects and observable properties (http://www.ghrsst-pp.org/SST-Definitions.html).

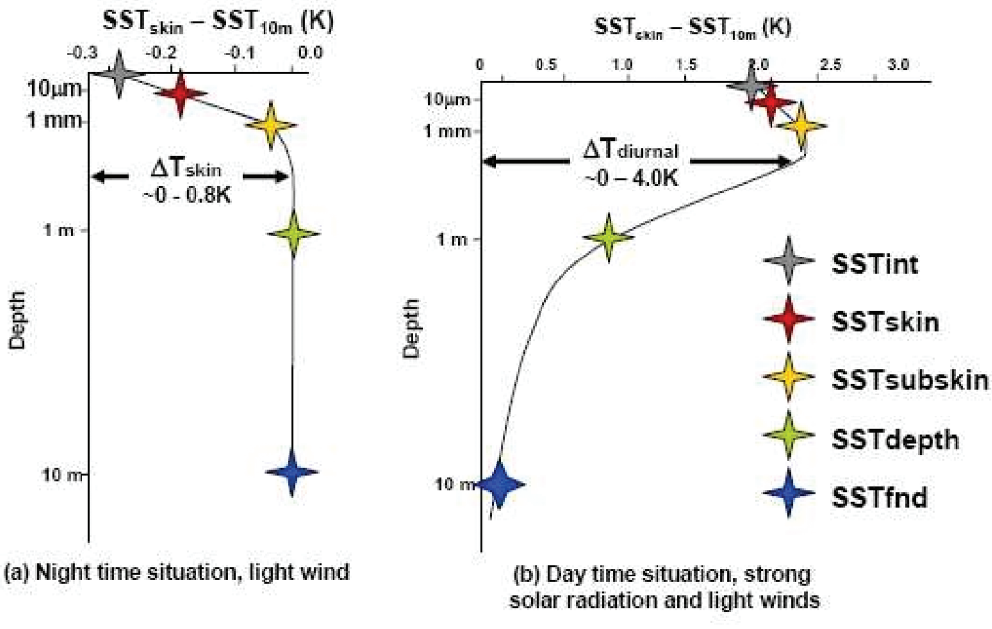

of NAVOCEANO's Global Area Coverage AVHRR L2P SST product (NAVOCEANO hereafter; May et al. 1998) this corresponds to single-swath files containing SST values, pixel location, as well as time of the observation, single sensor error statistics (SSES), bias and standard deviation of the temperature product against a matchup data base, rejection flags, confidence and proximity confidence flags.

NAVOCEANO SST retrievals are based on multi-channel SST (MCSST) and non-linear SST (NLSST) equations obtained through regression with buoy data (Walton et al. 1998; McClain et al. 1983). As such, the SST values most likely represent the temperature at a depth of 1 m. Similarly, the corresponding SSES estimates account for any temperature difference with buoy observations; the errors could be due to diurnal variation, cloud contamination, aerosol or even satellite problems.

The SST observations in this data-set are provided in a 8.8 km x 4.4 km resolution with estimated monthly bias and root mean square (RMS) error relative to buoys <0.1 K and <0.7 K respectively.

Observability

As an equivalent to the 1 m depth temperature, the NAVOCEANO L2P product is an approximation to the corresponding model variable, T_{5m}, required by OceanMAPS. This approximation is very good under sustained winds, but will lie further from foundation temperature for observations obtained under strong insolation and low winds. This is why collocated wind values are routinely used to accept/discard satellite SST products. Unfortunately, NAVOCEANO L2 products do not contain the auxiliary wind field, so a different criterion was developed to thin the data. This criterion was based on the distance in time between the observation being taken and that corresponding to local dawn: the closer these two times, the better approximation of the retrieved SST to T_{fnd}.

Processing the L2P files

The L2P files were processed for the benchmark period February-April 2008. The L2P data available for the period February to April 2008 come from three polar-orbiting satellites: NOAA17, NOAA18 and METOP-A. These provide approximately 40 single-swath files per day, with a per file size generally exceeding 100 MB over a global grid. The first task of this work was to read in the relevant information in daily grouped NAVOCEANO L2P GHRSST files and write this information in a smaller file that could contain only the fields required by BODAS at those points for which a measurement was available, leaving out fill-value points. The result was a daily file of size ~50 MB that contained the arrays of observed points, the corresponding observations, together with a set of fields characterising those observations.

Our intention was to process L2P observations as little as possible prior to ingestion into BODAS. BODAS has a preprocessing section (PREP hereafter) that reads in all available observations and their characteristics, then combines them into quality-controlled (QCd) super-observations with estimated error statistics.

The observation processing prior to BODAS call is carried out off-line, using a shell script. The script gathers all the files within a 24-hour window prior to a cut-off time (Fig. 2) and it:

- reads the relevant fields in each file;
- removes all fill-value pixels;
- makes the necessary conversions;
- corrects measurements for SSES biases;
- calculates the age of each observation relative to the closest pre-dawn time, taken as 0300;
- neglects observations taken more than six hours after/before foundation time, which is assumed to be at 0300 local time. This step could become redundant if wind products were available to filter for diurnal biased values. However, it also assures that the volume of data obtained for one day is manageable within allocated CPU times and keeps observations that are closest to foundation time.

Choice of satellites. Table 1 shows the equatorial crossing times for each of the polar-orbiting satellites providing the SST observations. A look at Table 1 identifies NOAA-18 as the satellite that crosses the equator at a descending time closest to 0300, that we have assumed to be foundation time. The closeness of NOAA-18 observations to foundation time is confirmed by Figs 3 to 5, which show the age of the observations gathered from each two-by-two combination of the three satellites. Although the three combinations produce similar coverage, a combination of NOAA-17 and NOAA-18

Table 1. Details of the three satellites providing observations for the L2P NAVOCEANO product within the period February-April 2008.

Satellite	*Type of data*	*Local equatorial crossing time*
MetOp-A	AVHRR	0930D/2130A
NOAA-18	AVHRR	0152D/1352A
NOAA-17	AVHRR	1025D/2225A

Fig. 2 Timeline of the production of daily files. L2P files are gathered in 24-hour time-windows previous to a chosen cut-off time.

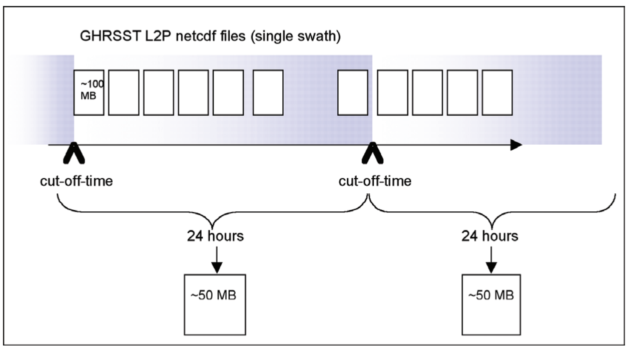

Fig. 3 Age of the observations obtained from satellites NOAA-18 and METOP-A with respect to local dawn time for 1 February 2008. Age is expressed as fraction of a day, in a time window of ±6 hours around foundation time, which we have assumed to be 0300.

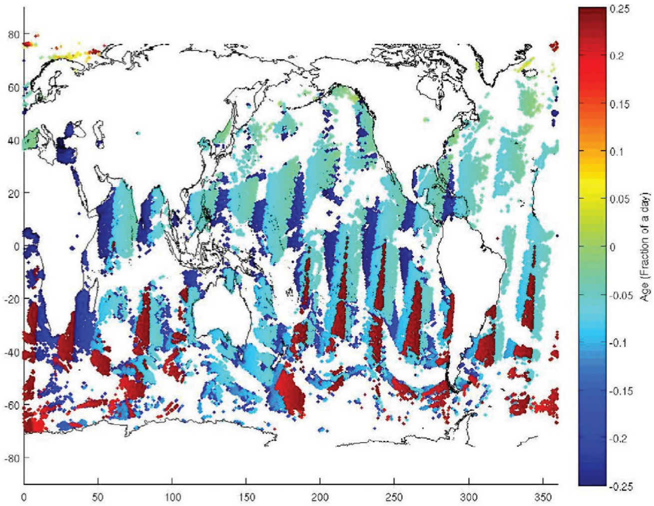

Fig. 4 Age of the observations obtained from satellites NOAA-17 and METOP-A with respect to local dawn time for 1 February 2008. Age is expressed in fraction of a day, in a time window of ±6 hours around foundation time, which we have assumed to be 0300.

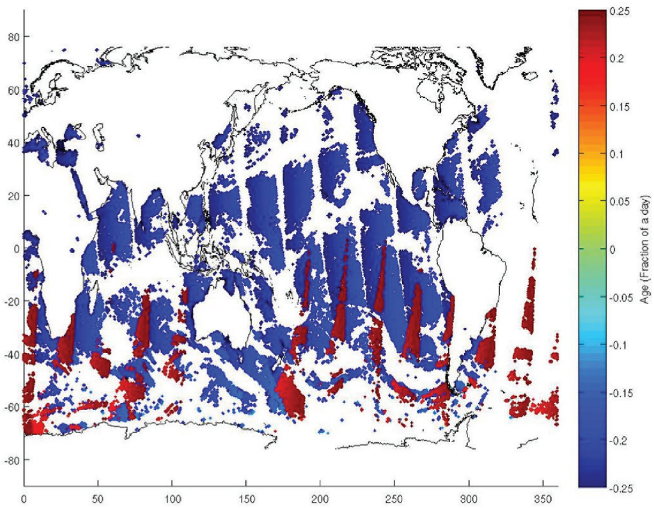

Fig. 5 Age of the observations obtained from satellites NOAA-17 and NOAA-18 with respect to local dawn time for 1 February 2008. Age is expressed in fraction of a day, in a time window of ±6 hours around foundation time, which we have assumed to be 0300.

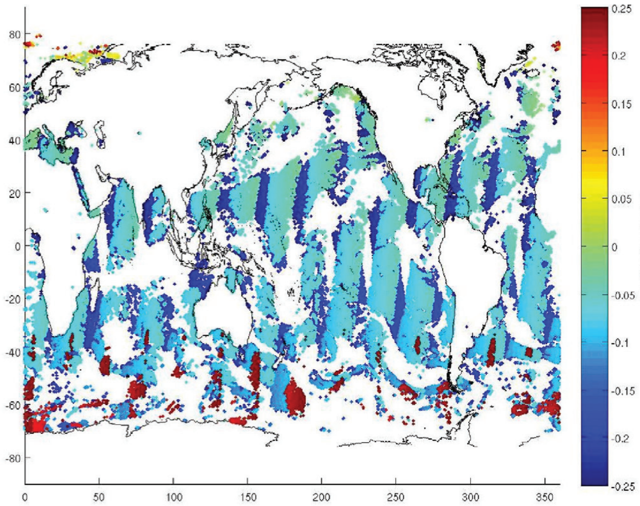

satellites appears as the most useful, based on an age criterion. Following these results and due to the high volume of incoming daily data, we chose to leave aside METOP-A, gathering only observations from NOAA-17 and NOAA-18 to produce the daily files intended for assimilation. Similar tests had been done to evaluate the impact of cut-off time in the age of the resulting daily product, with tests run for cut-off times 2000, 2200 and 0000 UTC. At present, this time is fixed to 2000 UTC, but it is most likely that the product's age will not be very sensitive to this parameter for the current coverage and equatorial crossing times of these satellites.

It is worth noting that METOP-A observations may be needed for dates on or after 6 July 2009, when NAVOCEANO discontinued production of the NOAA-17 GAC SST retrievals.

AMSR-E SST product

The Advanced Microwave Scanning Radiometer – Earth Observing System (AMSR-E), on board of the NASA Aqua satellite, measures sub-skin SST at approximately 1 mm depth. It provides daily global coverage at a resolution of 25 km and an accuracy of 1 K. The data were read in from a NetCDF file containing ascending and descending SST, which correspond to day and night observations respectively. Wind fields and observation times completed this information. For this study, all descending SST observations were used, the daytime observations being discarded.

Comparison of the satellite product against *in situ* data

Both the NAVOCEANO data and AMSR-E descending data were compared against *in situ* SST observations for the period February-April 2008. The *in situ* data were extracted from the Australian Data Archive for Meteorology (ADAM), an internal data archive system with web access.

AMSR-E and NAVOCEANO in collocated points

AMSR-E descending and NAVOCEANO data were compared to *in situ* data whenever both satellite data-sets had a data-point in the neighbourhood of a given *in situ* observation. This excluded comparison in cloudy regions, as AVHRR does not provide observations through clouds. Table 2 shows the mean, standard deviation and resulting RMS of the differences between the satellite and *in situ* data for all collocation points. Results show an overall higher misfit of AMSR-E to *in situ* data, mainly due to a stronger bias. Note that this shows warmer temperatures for both satellites, compared to those measured by the *in situ* data.

Additional statistics were calculated separately for all AMSR-E descending and NAVOCEANO data retained for the period February-April 2008. In this case the only requirement was that for each of the data-sets there was a collocated buoy observation (or vice versa). The following sections present some results for these separate statistics.

Influence of clouds on AMSR-E data quality

Based on particular cases where the error statistics of the model with respect to AMSR-E observations were higher in cloudy regions (not shown), we computed the statistics for all AMSR-E data and of that fraction of the data under clouds respectively. Table 3 shows the statistics of the differences between AMSR-E descending SST values and the corresponding *in situ* measurements for the AMSR-E data retained in February 2008. The results indicate a reduction of the cold bias of the satellite data-set under cloudy conditions which would actually result in an improvement of the data quality. On the other hand they also point at a degradation of the standard deviation values. The combination of these two effects results in an overall increase of the RMS for cloudy areas. However, this degradation is very small and not systematic (Fig. 6). Further study would require considering particular cases, which lies out of the scope of our present work.

Table 2. Statistics of the differences (SST_{sat} - SST_{buoy}) at satellite-buoy collocated points for February 2008. Similar results were obtained for March and April 2008.

	AMSR-E descending	*NAVOCEANO*
Mean difference	-0.2107	-0.0587
Standard deviation	0.6180	0.5124
RMS	0.6529	0.5157

Table 3. Mean, standard deviation and RMS error obtained from the differences between collocated AMSR-E and *in situ* measurements for February 2008. This figure is similar to those obtained for March and April 2008, with a higher mean departure for all AMSR-E data over the AMSR-E data in cloudy areas.

	all AMSR-E available data	*AMSR-E under cloud*
Mean	-0.1550	-0.1389
Standard deviation	0.6985	0.7194
RMS	0.7155	0.7327

Fig. 6 RMS time-series for all AMSR-E data with respect to collocated *in situ* measurements, for February 2008.

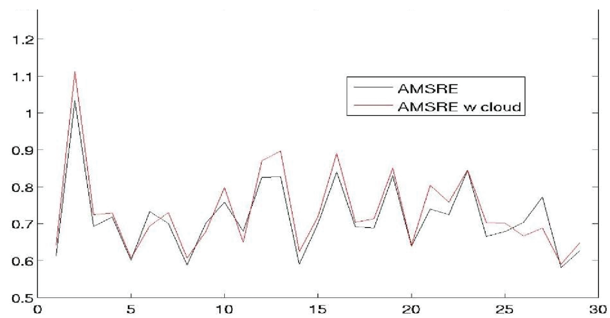

Assimilation experiments using BODAS

For each daily February 2008 forecast obtained by OceanMAPS, BODAS produced an analysis according to the expression:

$$x^a = x^f + P_{static}{}^f H^T (HP_{static}{}^f H^T + R)^{-1} (y^o - Hx^f), \qquad \ldots 1$$

where y^o represents the observation vector and H the observation operator, that translates the model state *x* to the locations and variable(s) comparable to the observation. In this case H consists of an interpolation that collocates observed and modelled SST. The analysis and forecast are represented by x^a and x^f respectively. $P_{static}{}^f$ is the background error covariance matrix, estimated from a set of static (i.e. not evolving) departures of the system with respect to a mean. For the current application, the ensemble consisted of 72 realisations of these departures, or 72 ensemble members, extracted from a spin-up run and intended to represent errors associated to time and space mesoscales.

The pre-processing component of BODAS, PREP, reads in the observations, performs quality controls and averages them onto a super-observation grid, also estimating the errors of the averaged super-observations from the individual observation error statistics. PREP was upgraded to be capable of ingesting the newly produced NAVOCEANO daily files. In order to assess the impact of the new data-set, three series of analyses were run: the first two would only assimilate NAVOCEANO and AMSR-E descending data respectively, the third would combine the two data-sets. Both series used previously obtained 24-hour OceanMAPS1.0b forecasts as background fields. The analyses thereby obtained were not used as the initial condition for subsequent forecasts and remained a collection of estimates from the chosen first guess estimates.

As the outcome of OceanMAPS, these first-guess estimates would already contain information from data-sets like AMSR-E, sea level anomaly (SLA) and *in situ* profiles, introduced in the system in prior assimilation steps. The following results are intended to assess the statistical impact of assimilation on already fairly good estimates of a field, and so are expected to present a small but noteworthy impact.

Figure 7 shows an example of the coverage of NAVOCEANO SST, that of AMSR-E descending observations and their combination. The coverage of the combined product is very satisfactory, although no observations are available for areas like Bass Strait in this example. Nonetheless, the incorporation of NAVOCEANO makes coastal areas 'visible' to the assimilation system, as is obvious in the Great Australian Bight and Gulf of Carpentaria for this case.

Innovation statistics

NAVOCEANO analyses. Figures 8 and 9 show respectively the mean and standard deviation for the background and analysis innovations obtained over all super-observation points gathered from the analysis series assimilating NAVOCEANO data. Background and analysis innovation are defined as the difference (y^o-Hx^f) and (y^o-Hx^a) respectively, that is the misfit to the observations y^o of their model equivalent, prior to (Hx^f) and after (Hx^a) assimilation. The figures show an overall decrease of both the mean and standard deviation of the analysis innovations compared to the background innovations. Figure 8 also shows a shift of sign in the mean innovation, that is positive prior to assimilation and negative for the analysed value. This appears to be due to a stronger correction of the positive innovations over that for the negative ones and it could be pointing at a bias in the analysis system: the background, the observations or the assimilation procedure itself. It is, however, possible for this to occur by the patterns of warm and cool anomalies and not just because of systemic problems.

The statistics shown earlier would discard the hypothesis of a bias in the observations, leaving the first guesses or the configuration of the assimilation system as the main possible contributions to that bias. Comparison of Figs 10 and 11, showing the histogram of the background analysis innovation and the distribution of the anomalies corresponding to the first 30 members of the static ensemble respectively, suggests that the relatively small ensemble spread could be linked to this asymmetry in the corrections. The underestimation of the background error covariances could, in effect, be leading to an under-fitting to the observations, with an analysis being drawn too close to the first guess.

Figures 12, 15 and 18 show the average SST increments introduced by BODAS throughout February 2008 when it assimilates NAVOCEANO, AMSR-E and the two products combined respectively. Comparison of Figs 12 and 15 shows the contribution of NAVOCEANO (Fig. 12) in coastal areas, for example in the Great Australian Bight, Bass Strait and Spencer Gulf. This contribution also appears in the analysis obtained using the combination of the two products (Fig. 18).

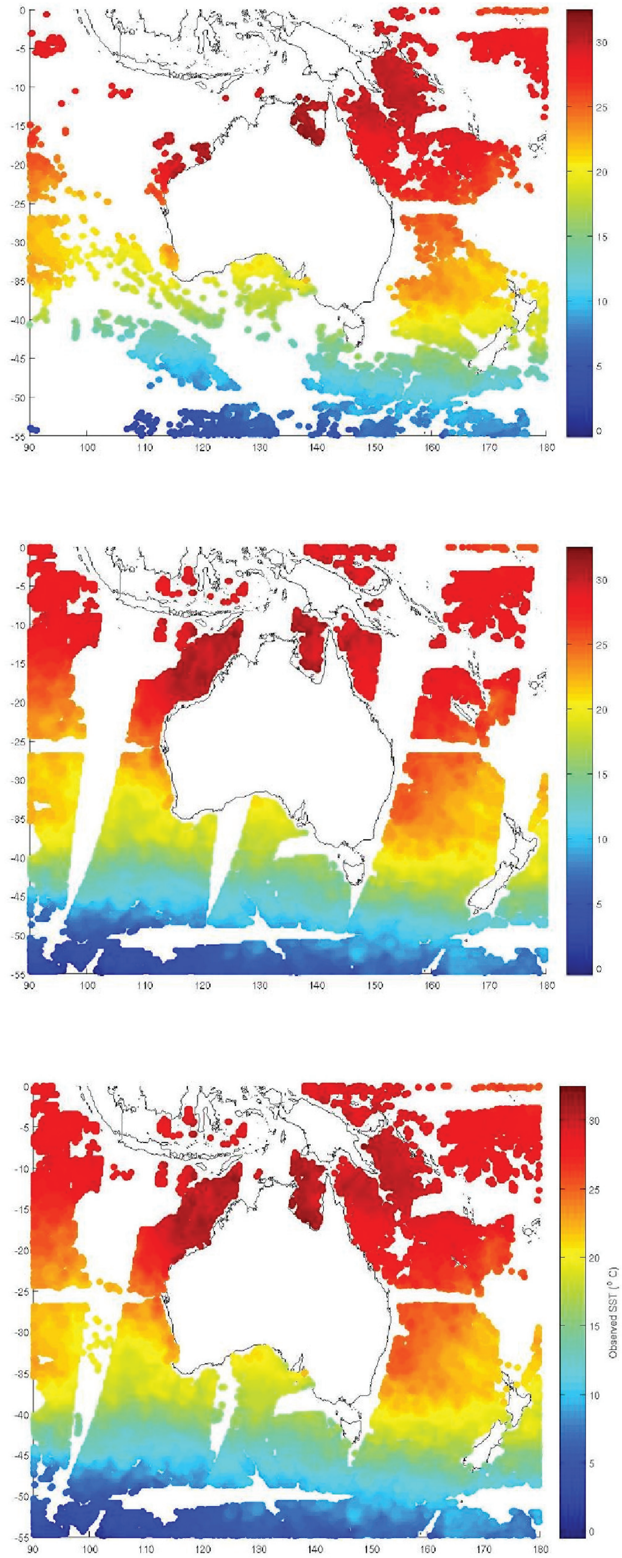

Fig. 7 Quality controlled NAVOCEANO (top), AMSR-E descending (centre) and their combination (bottom) at BODAS super-observation points for 3 February 2008. The combined product for this date presents very good coverage, and reaches some coastal areas (e.g. Spencer Gulf, Gulf of Carpentaria) through the NAVOCEANO contribution. AMSR-E does not observe within 50 km of the coast.

Fig. 8 Mean values of the background and analysis innovations for the analysis series assimilating NAVOCEANO-derived SSTs for February 2008. The computations have been made for all values together, as well as for positive values and negative values separately.

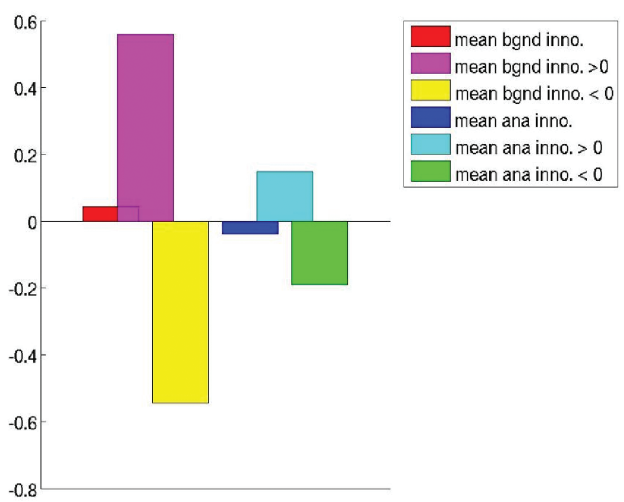

Fig. 9 Values of the standard deviation of the background and analysis innovations for the analysis series assimilating NAVOCEANO-derived SSTs for February 2008. The computations have been made for all values together, as well as for positive values and negative values separately.

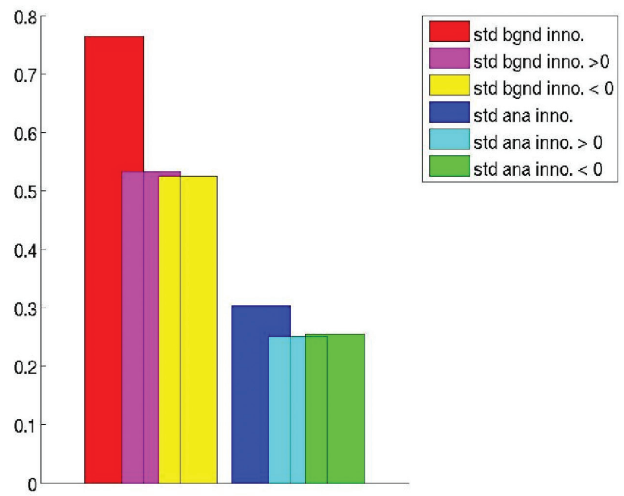

Fig. 10 Background innovation histogram for the analysis series assimilating NAVOCEANO-derived SSTs.

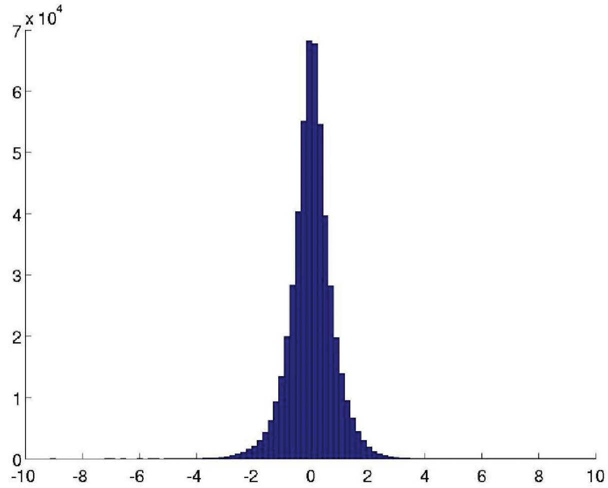

Fig. 11 Histogram for the ensemble anomalies of the first thirty members of the static ensemble used to estimate the background error covariances.

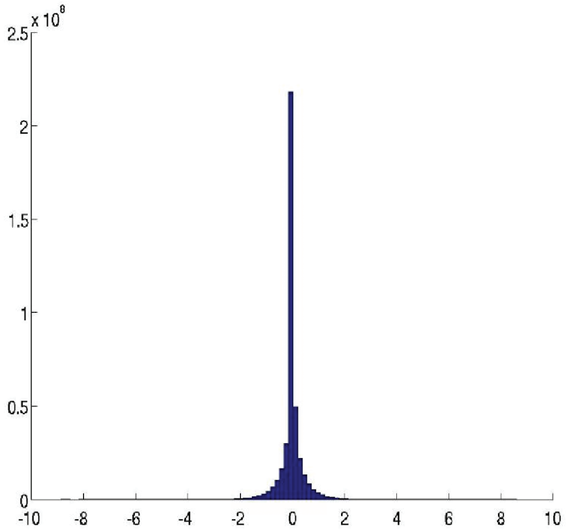

AMSR-E analyses. Figure 13 shows a mean background innovation of different sign to that illustrated in Fig. 8, which can be partly explained by the differences in the data statistics, AMSR-E presenting a greater negative bias. The mean analysis innovations, however, are closer to those found in Fig. 8. Figure 14 shows a behaviour similar to that in Fig. 9 for the standard deviation values.

NAVOCEANO and AMSR-E analyses. The combination of NAVOCEANO and AMSR-E descending data shows statistics very similar to those for the series assimilating AMSR-E data (Figs 16 and 17).

Figure 19 shows a Taylor diagram (Taylor 2001) presenting the correlation coefficient, centred RMS and standard deviation of the observational and analysed da-

Fig. 12 Average SST increments for February 2008 for the series of analyses assimilating NAVOCEANO SST products only. Ocean regions in white represent areas where the average increment is zero. This can be due to cancellation between increments with compensating values, or to lack of observations.

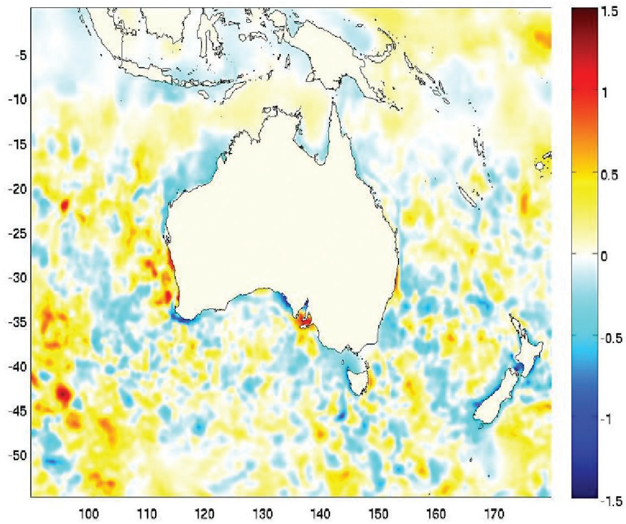

Fig. 13 Mean values of the background and analysis innovations for the analysis series assimilating AMSR-E-derived SSTs for February 2008. The computations have been made for all values together, as well as for positive values and negative values separately.

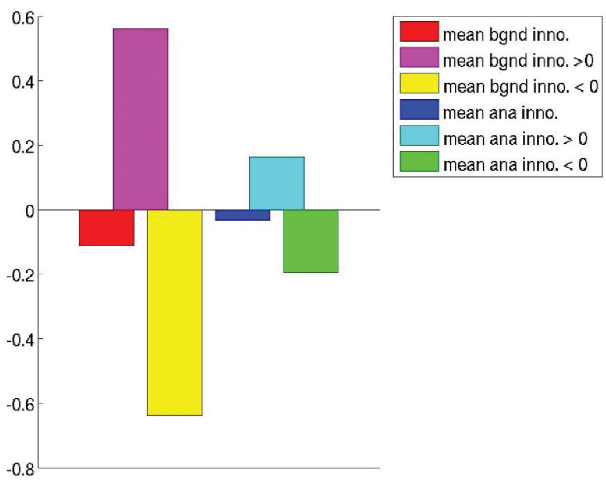

Fig. 14 Values of the standard deviation of the background and analysis innovations for the analysis series assimilating AMSR-E-derived SSTs for February 2008. The computations have been made for all values together, as well as for positive values and negative values separately.

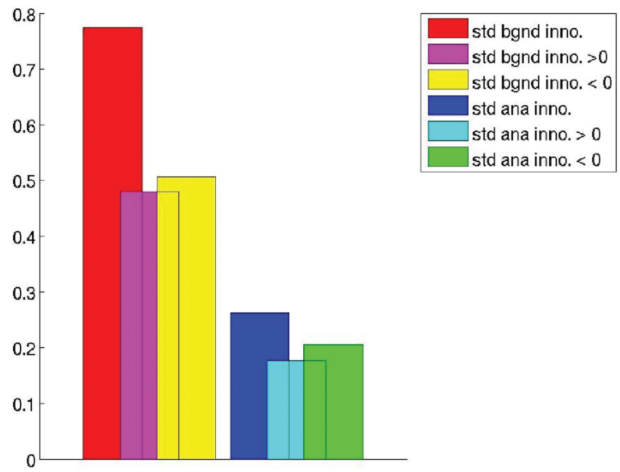

Fig. 15 Average SST increments for February 2008 for the series of analyses assimilating AMSR-E SST products only. Ocean regions in white represent areas where the average increment is zero. This can be due to cancellation between increments with compensating values, or to lack of observations.

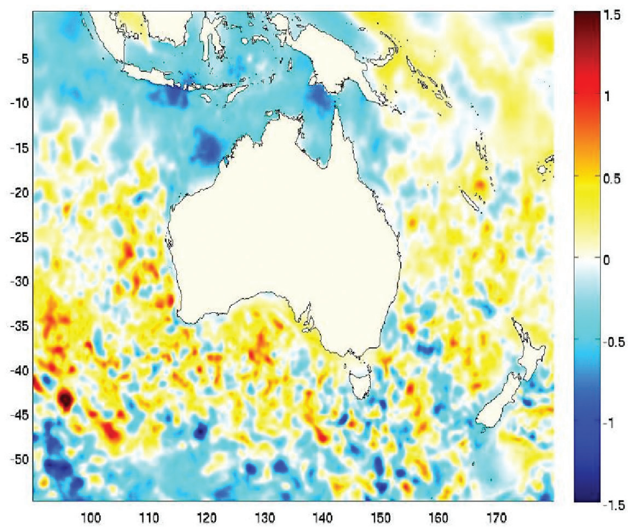

ta-sets with respect to the *in situ* data-set. This diagram shows that *in situ* data are most closely correlated with satellite observations, but the BODAS analysis shows a lower RMS difference. This could suggest that the combination of observations with a dynamically consistent background state is able to represent the variability of the system more faithfully. We will be addressing this question in future studies.

Fig. 16 Mean values of the background and analysis innovations for the analysis series assimilating AMSR-E and NAVOCEANO combined products for February 2008. The computations have been made for all values together, as well as for positive values and negative values separately.

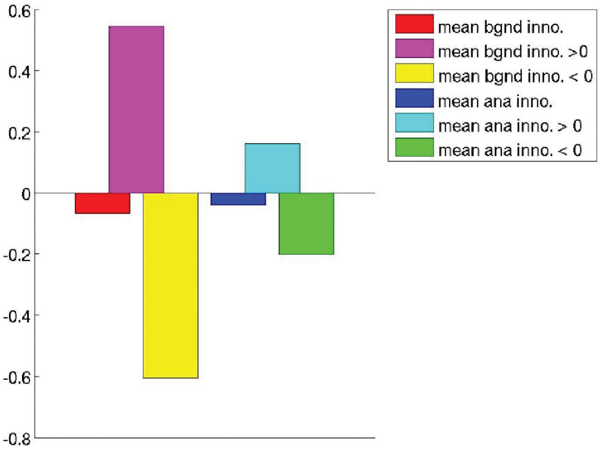

Fig. 17 Values of the standard deviation of the background and analysis innovations for the analysis series assimilating AMSR-E and NAVOCEANO combined products for February 2008. The computations have been made for all values together, as well as for positive values and negative values separately.

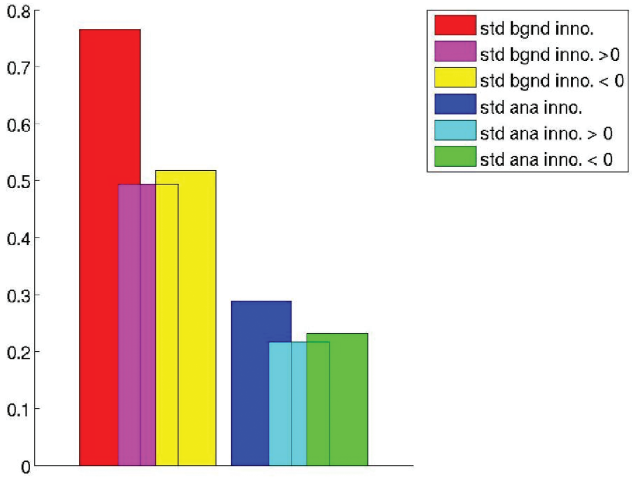

Fig. 18 Average SST increments produced by assimilation of AMSR-E and NAVOCEANO observations for February 2008. Ocean regions in white represent areas where the average increment is zero. This can be due to cancellation between increments with compensating values, or to lack of observations.

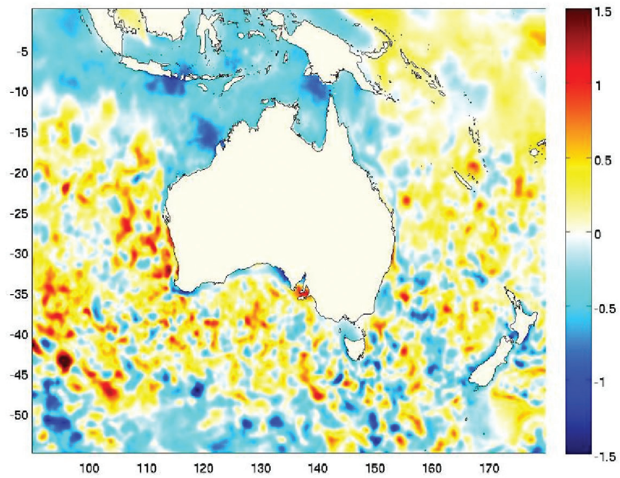

Fig. 19 Taylor diagram that synthesises statistical information for *in situ* data (red), NAVO observations (dark blue), AMSR-E descending observations (magenta) and the three analysis series performed with BODAS assimilating NAVOCEANO, AMSR-E and their combination respectively (green). Only the 'BODAS' label has been left for the three corresponding points in the graph for legibility. The radial distance from the origin is proportional to the standard deviation of the corresponding field. The centred RMS difference between the observational and analysed data-sets with respect to the reference (*in situ*) data-set is proportional to their distance in the same units as the standard deviation (° C). The azimuthal position of the different fields gives their correlation with the *in situ* data-set.

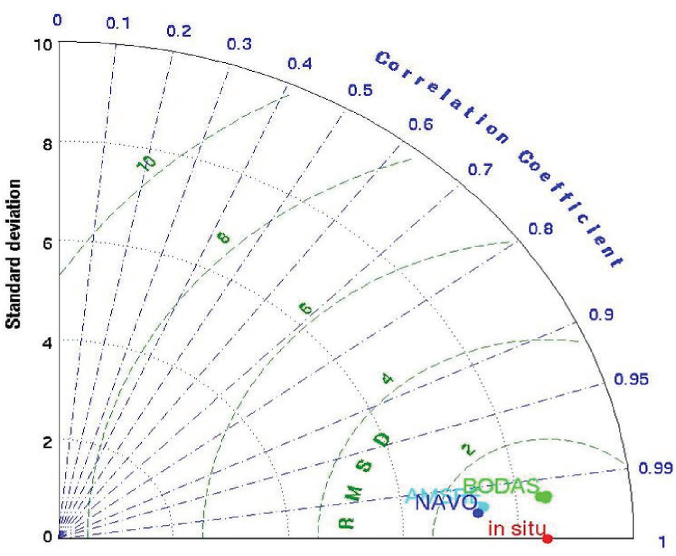

Discussion and conclusions

This paper has presented the implementation of a high resolution AVHRR SST data stream into the BLUElink Ocean Data Assimilation System. NAVOCEANO's Global Area Coverage AVHRR L2P SST product was processed to produce daily files of global SST. An age criterion was used to select the data by which only the observations within six hours of 0300 would be selected. A consequence of this choice may be the higher contribution of satellite NOAA-18 to the new BODAS data stream. The statistical characteristics of the data-set and of that previously ingested into BODAS, with respect to available *in situ* data show smaller bias and standard deviation errors for the new data stream. This provides higher resolution and brings observations to coastal areas, which are data-void for the pre-existing data stream. The main shortcoming of the new data-set is the absence of observations under clouds, resulting in variable coverage. Assimilation of the two data-sets separately and combined has shown an obvious improvement of the error statistics in all cases. There appears to be a common distribution of the analysis innovation errors for the analyses assimilating AMSR-E data only and those assimilating a combination of AMSR-E and NAVOCEANO. Although combining the two products does not appear to improve the analysis innovation statistics, it improves coverage, resulting in a better final estimate of the physical field over the domain. The availability of two SST data streams also improves the robustness of the prediction system.

This work points at open questions regarding the possibility of a bias in the prediction system, with a stronger correction for temperatures warmer than observed. A possible source of bias is the choice of the ensemble. This is a very interesting question, that needs consideration of the different time and space scales involved in the system, which will vary depending on the region, processes and fields considered. From another perspective, this could well be the opportunity to couple a bias correction scheme to the assimilation system and assess the impact on its behaviour.

Acknowledgments

This research was supported by the BLUElink project, Bureau of Meteorology, CSIRO and the Royal Australian Navy. We wish to thank Drs Jean-Francois Cayula and Doug May (NAVOCEANO) and Dr Mark Filipiak (University of Edinburgh) for their advice and help with the assimilation of GHRSST NAVOCEANO AVHRR data into BODAS. The authors are also grateful to Dr Justin Freeman for the implementation of a parallel version of BODAS and Dr Paul Sandery for valuable input.

References

Brassington, G.B., Pugh, T.F., Spillman, C., Schulz, E., Beggs, H., Schiller A. and Oke, P.R. 2007. BLUElink> development of operational oceanography and servicing in Australia. *J. Res. and Prac. Info. Tech., 39*, 151-64.

May, D.A., Parmeter, M.M., Olszewski, D.S. and McKenzie, B. 1998. Operational processing of satellite sea surface temperature retrievals at the naval oceanographic office. *Bull. Am. Met. Soc., 79*, 397–407.

McClain, E.P., Pichel, W., Walton, C., Ahmad, Z. and Sutton, J. 1983. Multi¬channel improvements to satellite-derived global sea surface temperatures. *Adv. Space Res., 2(6)*, 43–7.

Oke, P.R., Brassington, G.B., Griffin D.A. and Schiller, A. 2008. The Bluelink ocean data assimilation system (BODAS). *Ocean Modelling, 21*, 46-70.

Soloviev, A. and Lukas, R. 2006. *The near-surface layer of the ocean. Structure, dynamics and applications*. Springer, 572 pp.

Taylor, K.E. 2001. Summarizing multiple aspects of model performance in a single diagram. *J. Geophys. Res., 106*, D7, 7183-92.

Walton, C.C., Pichel, W.G. and Sapper, J.F. 1998. The development and operational application of nonlinear algorithms for the measurement of sea surface temperatures with the NOAA polar-orbiting environmental satellites. *J. Geophys. Res., 103,* 27999–28012.